ESLAB #53: The *Gaia* Universe
Edited by J.H.J. de Bruijne

Synergies between *Gaia* and LISA missions for Galactic multi-messenger studies

Valeriya Korol[1] and Elena M. Rossi[1]

[1]Leiden Observatory, Leiden University, PO Box 9513, 2300 RA, Leiden, the Netherlands

Abstract

Ultra-short period Galactic binaries are unique multi-messenger tracers of the Milky Way. They can be detected in large numbers through electromagnetic radiation by *Gaia* and through gravitational waves by the upcoming LISA mission. First, we revise the current census of known multi-messenger Galactic binaries by computing their GW signals using updated distances from the *Gaia* Data Release 2. Our work confirms thirteen guaranteed multi-messenger sources: nine AM CVns, three detached double white dwarfs (DWD) and one hot subdwarf. Next, we forecast the detection prospects for DWDs with both *Gaia* and LISA using a binary population synthesis technique. We predict respectively hundreds and tens of thousands detections by *Gaia* and LISA, with an overlap of several tens. We show that synergies between *Gaia* and LISA observations of DWDs allow the study of the Milky Way baryonic structure. The success of this synergy is due to LISA's ability to localise binaries through virtually the whole Galactic plane, thus mapping its shape. While observations of LISA's electromagnetic counterparts observed by *Gaia* yield the information on their motion; tracing the underlying total enclosed mass. We envisage that multi-messenger observations will ensure the best science return of the LISA mission for Galactic studies.

1 Introduction

Gaia is the ongoing ESA mission, that currently scanning our Galaxy registering brightness, sky position and motion for billions of stars across the Milky Way (Gaia Collaboration *et al.*, 2016, 2018). Laser Interferometer Space Antenna (LISA) is the future ESA mission, that besides probing high-redshift cosmology (Caprini *et al.*, 2016; Tamanini *et al.*, 2016, e.g.,) and testing the theory of General Relativity in the strong gravity regime (e.g., Barausse *et al.*, 2016; Berti *et al.*, 2016; Brito *et al.*, 2017), will also detect a large number of Galactic gravitational wave (GW) sources (e.g. Nelemans *et al.*, 2004; Ruiter *et al.*, 2010; Nissanke *et al.*, 2012). An overlap of several tens to a few hundred of sources is expected between the two missions (e.g., Korol *et al.*, 2017; Breivik *et al.*, 2018).

Multi-messenger synergies between the *Gaia* and LISA missions are possible by exploiting ultra-short period ($<$ 1 h) Galactic binaries composed of compact stellar remnants: white dwarfs, neutron stars and black holes. The most numerous of which are expected to be detached double white dwarfs (DWDs) and AM CVn stars (Nelemans *et al.*, 2001; Ruiter *et al.*, 2010; Nissanke *et al.*, 2012; Korol *et al.*, 2017; Breivik *et al.*, 2018). Other binaries such as white dwarf - neutron star, double neutron stars and double black holes are expected to be significantly less abundant (Nelemans *et al.*, 2004; Tauris, 2018; Lamberts *et al.*, 2018). Therefore, here we mainly focus on binary systems in which both components are white dwarfs: DWDs and AM CVns. Although quite faint, these binary systems are straightforward to detect with *Gaia*. For example, a few hundred DWDs are expected to be discovered by *Gaia* as eclipsing sources (Korol *et al.*, 2017).

The strength of multi-messenger observation reside in the fact that GWs provide very different (but complementary) information compared to what can be deduced from electromagnetic (EM) observations. In general, from EM data one can learn the chemical composition and the temperature of an astronomical object, while from GWs one can recover its mass and the distance. More specifically for Galactic studies, LISA's capability to directly determine luminosity distance[1] (typically difficult to derive directly from optical observations for such faint sources) for a large number of Galactic GW sources as well as the fact that GWs are unaffected by stellar dust will enable a 3D localisation of the GW source in the Galaxy. On the other hand, large error bars on the sky position typical of GW observations (compared to EM ones) does not allow to follow the motion of a source on the sky. Therefore, numerous resolved GW signals (but also unresolved population) will provide a tomographic picture of the Galaxy; while, the full picture emerges jointly with optical kinematic properties of EM counterparts complementing the positional information from GWs. In this way LISA's observations combined with those from *Gaia* will unveil both the shape and total dynamical mass of the Galaxy.

2 Guaranteed multi-messenger binaries

A subset of the known ultra-short period Galactic binaries (i.e. those discovered using standard EM detection techniques), that are predicted to emit strong GW signals, represent a sample of *guaranteed* LISA sources. They are also called "LISA verification binaries", because the a priori knowledge of their GW signal can be used to validate LISA data (e.g., Ströer & Vecchio, 2006). The list of the currently known LISA verification binaries is mainly composed of DWD and AM CVn systems.

To forecast GW signals for LISA verification binaries, pre-

[1]Note, that this is true only for GW sources with measurable frequency derivative.

cise knowledge of the binary components masses, orbital inclinations and distance is required. Masses can be derived from EM observation by combining optical spectroscopy and photometry with the geometry of the system. The orbital inclination can be only derived in favourable situations. For example, when the binary is edge-on and eclipsing (e.g., Brown *et al.* 2011). However, generally inclination is a poorly constrained parameter. So far, distances remained the most uncertain of the parameters. Only a handful of the known AM CVn systems have parallaxes measured by the Hubble Space Telescope (Roelofs *et al.*, 2007; Nelemans *et al.*, 2004; Thorstensen, 2003; Thorstensen *et al.*, 2008). While, for the majority of systems the distances are estimated indirectly, for example, via the comparison with stellar models (e.g., Brown *et al.* 2016). The second *Gaia* data release (DR2, Gaia Collaboration *et al.*, 2018) for the first time provided parallax measurements for many of the candidate LISA verification sources (Kupfer *et al.*, 2018).

We analyse 52 known ultra-short period binaries present in the *Gaia* DR2 catalogue. We find that for 45% of the sample, parallaxes are measured with a fractional error of < 0.2. Thus, to convert *Gaia* parallaxes into distances we use a probability-based Bayesian inference approach outlined in (e.g., Bailer-Jones, 2015; Luri *et al.*, 2018). This method requires an assumption on the true distribution of the distances to ultra-compact Galactic binaries, called a Prior. In particular, this assumption is especially relevant when fractional errors on parallax are large ($\sigma_\varpi/\varpi > 0.2$; Bailer-Jones, 2015). For our study we adopt an exponentially decreasing volume density prior (Kupfer *et al.*, 2018, equation 3), that implies a constant space density for binaries with $d << L$ with d being the distance from us and L being a scale length of the prior, and an exponential drop for $d >> 2L$, where $2L$ corresponds to the peak of the distribution. The choice for the value of $L = 400$ pc is fine-tuned on the mock population of Galactic GW sources from Korol *et al.* (2017). Our results are reported in Kupfer *et al.* (2018, table 2).

Distances derived from *Gaia* parallaxes make it possible to compute the characteristic strain (i.e., the amplitude of GWs) as (e.g., Maggiore, 2008):

$$\mathcal{A} = \frac{2(G\mathcal{M})^{5/3}}{c^4 d}(\pi f)^{2/3}, \qquad (1)$$

where $\mathcal{M} = (m_1 m_2)^{3/5}/(m_1+m_2)^{1/5}$ is the so-called chirp mass with m_1 and m_2 being the binary component masses; and $f = 2/P$ is the GW frequency with P being binary orbital period. To compute the GW signals, the signal-to-noise ratios (SNR) and the noise of the detector including the foreground from unresolved Galactic sources we use the method described in Shah *et al.* (2012). Figure 1 illustrates GW amplitudes for the verification binaries in comparison with the LISA noise curve. For this calculation we adopt the latest mission design as approved by ESA and a nominal mission duration of 4 years (Amaro-Seoane *et al.*, 2017). Our estimates confirm thirteen guaranteed LISA sources with SNR$\geq$ 5. Most of which are of AM CVn type: HM Cnc, V407 Vul, ES Cet, AM CVn, SDSS J190817.07+394036.4 (SDSS J1908), SDSS J135154.46-06309.0 (SDSS J1351) HP Lib, CR Boo, and V803 Cen (Strohmayer, 2004; Ramsay *et al.*, 2005; Espaillat *et al.*, 2005; Roelofs *et al.*, 2006, 2007; Kupfer *et al.*, 2015; Green *et al.*, 2018). Three are detached DWDs: SDSS J065133.34+284423.4 (SDSS J0651), SDSS J093506.92+441107.0 (SDSS J0935) and

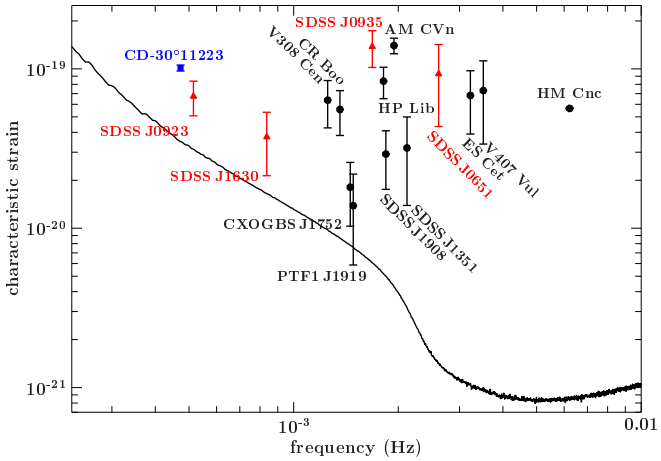

Figure 1: Frequency and characteristic strain of the LISA verification binaries with SNR$\geq$ 5. Black circles are AM CVn systems, red triangles correspond to DWDs and the blue square is the hot subdwarf binary. The black solid line represents LISA sensitivity curve from Amaro-Seoane *et al.* (2017). Note, that we do not show the error bar for HM Cnc because of large uncertainty on the distance. Figure adopted from Kupfer *et al.* (2018).

SDSS J092345.59+302805.0 (SDSS J0923) (Brown *et al.*, 2011; Kilic *et al.*, 2014). Finally, the last one is a hot subdwarf (i.e., He star + white dwarf) CD−30°11223 (Geier *et al.*, 2013), that for the first time was confirmed as a LISA verification source. Note that, thanks to *Gaia* parallaxes, it is possible to predict the GW amplitude with an accuracy better than 5% for CD−30°11223 and 10% for AM Cvn, making these systems ideal for testing LISA's performance. Note also that HM Cnc, expected to be the strongest GW source among known verification binaries, was not observed by *Gaia*. Thus, for our calculations we assume its distance to be 5 kpc (for discussion see Kupfer *et al.*, 2018). Because of the large uncertainty on the distance we do not represent the respective error bar for its characteristic strain in Fig.1.

The current sample of guaranteed LISA sources is limited in number, and is also incomplete and biased. In particular, AM CVn type systems are over-represented as they are brighter in EM radiation. Furthermore, the surface density of verification binaries is expected to trace the density of the overall stellar Galactic population, and, thus, to peak near the Galactic plane. However, the majority of the known systems are located in the Northern hemisphere, highlighting a clear observational bias. A more unbiased sample will be assembled in the years preceding the LISA's launch by ongoing and upcoming large scale optical surveys such as ZFT (Zwicky Transient Facility, Bellm, 2014), BlackGem (Bloemen *et al.*, 2015), GOTO (Gravitational-wave Optical Transient Observer Steeghs, 2017), *Gaia* and LSST (Large Synoptic Survey Telescope, LSST Science Collaboration *et al.*, 2009). We further discuss the future prospects for the last two surveys in Sect. 3.

3 Future multi-messenger opportunities

Here we forecast the size and the properties of the future multi-messenger EM+GW sample focusing on detached

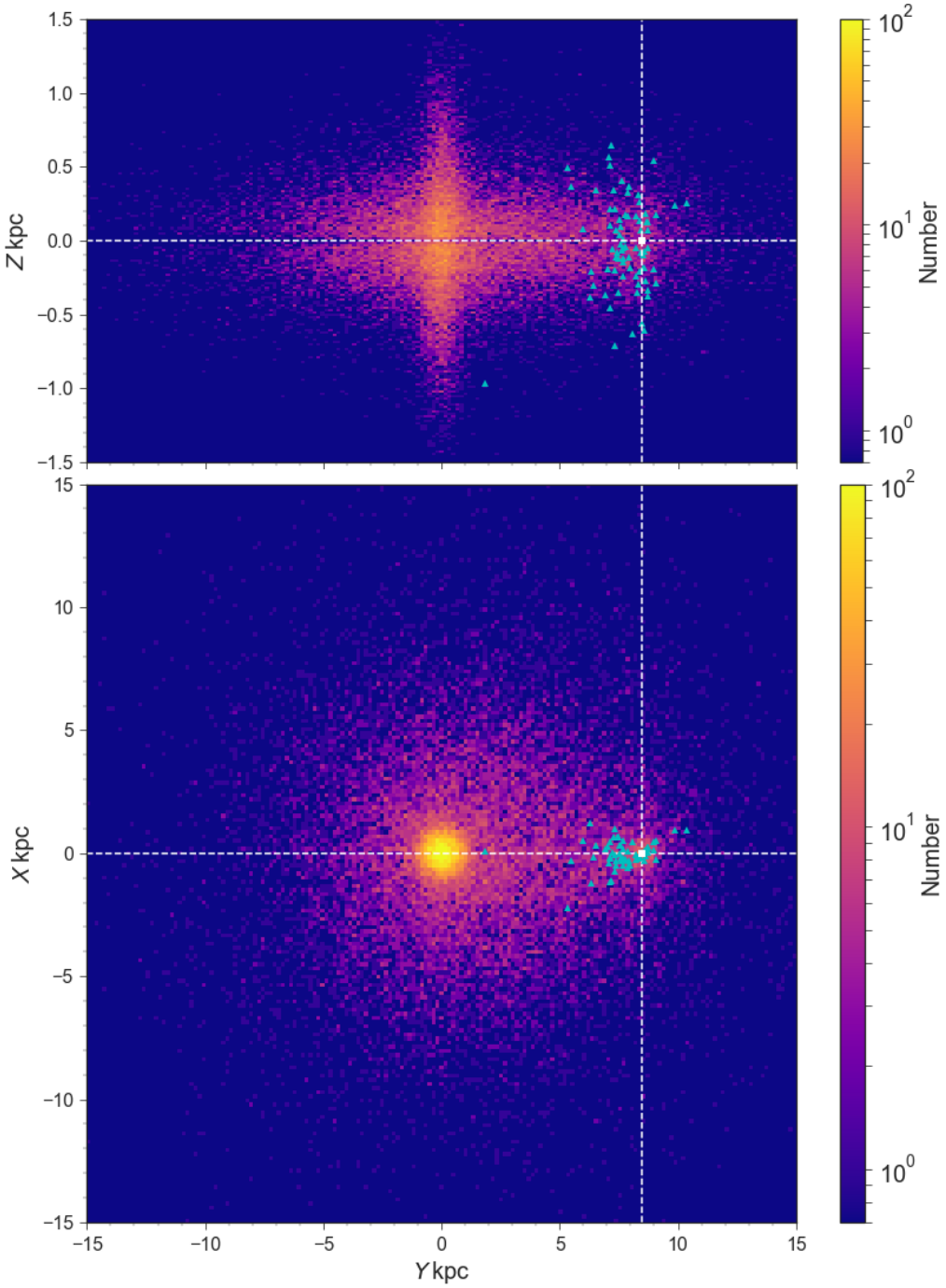

Figure 2: Source-count maps of DWDs detected by LISA (SNR$>$ 7) in the Galactocentric Cartesian coordinate system: in the $Y-Z$ plane (top panel) and in the $Y-X$ plane (bottom panel). The white square identifies the position of the Sun in our mock Galaxy, $(0, 8.5\mathrm{kpc}, 0)$. Blue triangles represent the position of EM counterparts detected with *Gaia* and/or LSST. Figure adopted from Korol *et al.* (2019).

DWDs only.

We model a mock Galactic population of DWDs using the binary population synthesis code SeBa developed by Portegies Zwart & Verbunt (1996), and fine-tuned for DWDs by Nelemans *et al.* (2001); Toonen *et al.* (2012). We assume a simplified Milky Way potential composed of an exponential stellar disc and a spherical central bulge. For the detailed description of the Milky Way we refer the reader to Korol *et al.* (2019). We distribute DWDs in the bulge and in the disc according to the star formation rate computed numerically by Boissier & Prantzos (1999) assuming the current age of the Galaxy to be 13.5 Gyr. For each binary we assign an inclination angle ι, drawn from a uniform distribution in $\cos\iota$. Thus, each binary in our catalogue is characterised by seven parameters: m_1, m_2, P, the inclination angle with respect to the line of sight ι, the Galactic latitude l and longitude b, and d. Given theses seven parameters and randomising over the initial orbital phase and polarisation angle, we compute DWD GW signals using the Mock LISA Data Challenge pipeline (e.g., Littenberg *et al.*, 2013), designed for the analysis of a large number of GW sources simultaneously present in the data.

We find that out of 2.6×10^7 DWDs in our mock catalogue, about 2.6×10^4 ($\sim 0.1\%$) can be individually resolved by LISA with a SNR$\geq$ 7 in 4 years of mission. The spacial distribution of LISA detections covers the whole surface of the stellar disc including the inner part of the disc, Galactic centre and reaching the opposite edge of the Galaxy. This is illustrated in Fig. 2. About 30% of the LISA detections have sky positions determined to a few deg^2 and distances determined within 30%, thus these binaries will be quite well localised in the Galaxy. Their 3D localisation allows the determination of the disc and bulge scale radii to a few per cent precision and the disc scale height up to ten per cent (Korol *et al.*, 2019). These results prove that GW data alone can elucidate on the Milky Way's structure in an unbiased way.

To fully unleash the potential of GW observations for Galactic studies, EM counterparts are required. To estimate the number of optical counterparts to LISA's detections one can search in large optical catalogues for periodically variable sources with a frequency and within an area on the sky matching those provided by LISA. To assess this possibility we focus only on edge-on binaries, which are easy to identify in the optical band as eclipsing sources. For simplicity we neglect gravitational distortion and mutual heating of the binary components. Neglecting these effects limits our search to systems with inclination angles $\sim 90^\circ$, meaning that our results represent a lower limit for EM detections.

We consider two optical surveys, which, by the time LISA will be operational, are expected to provide the largest Galactic stellar catalogues: *Gaia* (Gaia Collaboration *et al.*, 2018) and LSST (LSST Science Collaboration *et al.*, 2009). We compute bolometric and *ugriz*-Sloan magnitudes of DWDs using the white dwarf cooling curves of pure hydrogen atmosphere models (Holberg & Bergeron, 2006; Kowalski & Saumon, 2006; Tremblay *et al.*, 2011, and references therein). The absolute magnitudes are converted to observed magnitudes (e.g. for the Sloan r band) as

$$r_{\rm obs} = r_{\rm abs} + 10 + 5\log d + 0.84A_{\rm V}, \qquad (2)$$

where $0.84A_{\rm V}$ is the extinction in the Sloan r band and $A_{\rm V}$ is the extinction in the V band. To compute the value of $A_{\rm V}$ at the source position, defined by the Galactic coordinates (l, b) and the distance d, we use

$$A_{\rm V}(l,b,d) = A_{\rm V}(l,b)\tanh\left(\frac{d\sin b}{h_{\rm max}}\right), \qquad (3)$$

where $A_{\rm V}(l,b)$ is the integrated extinction in the direction defined by (l,b) from Schlegel *et al.* (1998), $h_{\rm max} \equiv \min(h, 23.5\times\sin b)$ and $h = 120$ pc is the Galactic scale height of the dust (Jonker *et al.*, 2011). Finally, to compute *Gaia* G magnitudes we apply a colour-colour polynomial transformation with coefficients derived for WDs by Carrasco *et al.* (2014).

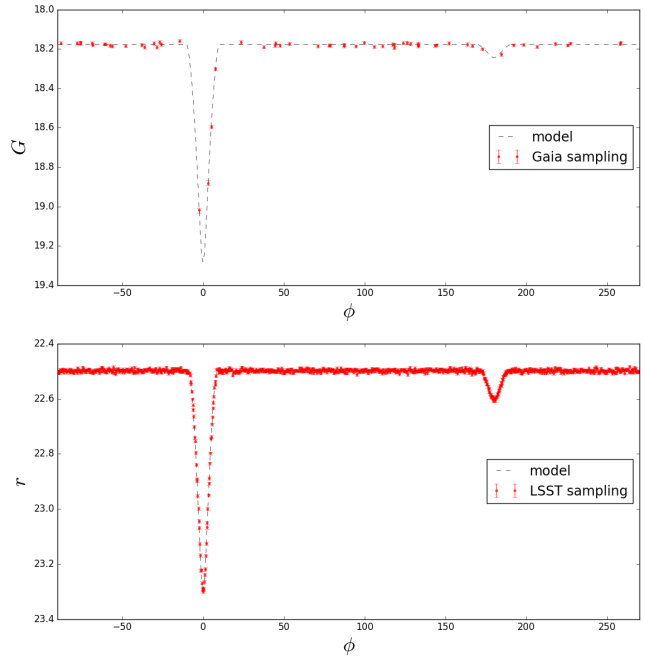

Figure 3: Phase folded light curves sampled with *Gaia* (top pannel) and LSST (bottom pannel). Figure adopted from Korol *et al.* (2017).

Next, we simulate the theoretical light curves of DWDs detectable with LISA using a simple geometrical model that provides the flux of a binary for a given orbital phase. We sample the theoretical light curves using the predicted *Gaia* observations obtained with the *Gaia Observation Forecast Tool*[2]. For the LSST sampling we use the anticipated regular cadence of 3 days over the nominal ten-year life span of the mission. Two examples of theoretical light curves (dashed black line) and the obtained mock observations (red circles) are represented in Fig. 3. For each light curve we compute 100 realisations of its sampling with observations by randomising over the initial orbital phase, and we define the probability of detection as the number of times the light curve was classified as detected out of 100. Our estimates for these two surveys indicate that the deep magnitude limit of 21 for *Gaia* and 24 for the LSST enables the detection of respectively hundreds and thousands of DWDs as eclipsing (Korol *et al.*, 2017). The distribution of orbital periods of these binaries

[2]http://gaia.esac.esa.int/gost/

ranges from about 10 min to 30 hours (see Korol *et al.*, 2017, figure 6).

About 80 DWDs constitute to a multi-messenger sample being detected by *Gaia* and/or LSST and also by LISA. Hereafter we call them EM counterparts. We represent LISA EM counterparts in Fig. 2 with blue triangles. Although the obtained multi-messenger sample is mostly confined within a few kpc, it is several times larger than the current sample described in Sect. 2, and will be important for maximising the scientific return of GW observations. For example, by adopting accurate EM sky positions, one can improve uncertainties from GW observations by a factor of a few (Shah *et al.*, 2012). While adopting binary orbital inclination or change in orbital period ($\dot{P}$) lead to an improvement by a factor of a few tens (Shah *et al.*, 2013). More importantly, the obtained GW+EM sample will enable multi-messenger *Galactic* astronomy and provide a new view of the Milky Way.

Using a geometrical argument we compute mock *Gaia* and LSST observations of DWD parallaxes, ϖ, and proper motions, μ, for a given position in our synthesis Galaxy (see Korol *et al.*, 2019, section 5). The respective errors, σ_ϖ and σ_μ, are obtained according to prescriptions from the Gaia Collaboration *et al.* (2016) for Gaia, and from the LSST Science Collaboration *et al.* (2009) for LSST. For each DWD we combine GW distances and parallaxes though Bayes theorem by using the probability density distribution for the distance obtained from GW data as the Likelihood, and the probability density distribution for the distance from parallaxes (as described in Sect.2) as the Prior. In this way we improve our distance estimates and compute the observed cylindrical distance of DWDs from the Galactic Centre, $R = \sqrt{R_0^2 + d^2 - 2R_0 d\cos l}$ with R_0 being the distance of the Sun from the Galactic centre. Using mock proper motions we derive the rotation speed of DWDs as (e.g., Sofue, 2017):

$$V_{\rm circ}(R) = -\frac{R}{d - R_0\cos l}(\mu d + V_0 \cos l), \qquad (4)$$

where V_0 is the rotation speed of the Sun, that we assume as known. Finally, we combine the obtained Galactocentric distances and rotation speeds into a rotation curve represented in Fig. 4. Note, that when computing $V_{\rm circ}$ we also account for the velocity dispersion by numerically computing velocity moments using equations (5.6) and (5.7) from Korol *et al.* (2019).

In general, the rotation curve traces the underlying total (baryonic + dark) enclosed mass of the Galaxy (e.g., Binney & Tremaine, 2011). Using prior assumptions on structural parameters such as the scale radii of the Galactic components, one can recover their masses. We fit the mock data with the total rotation curve corresponding to our Milky Way model, which we compute as $V^2_{\rm circ}(R) = Rd\Phi/dR$ with Φ being the total potential. We perform the fit with a MCMC code fixing scale radius of the bulge $r_{\rm b}$ and disc $R_{\rm d}$, and the disc scale height $Z_{\rm d}$ to the values obtained by fitting the density distribution of all LISA detections, and leaving free the remaining parameters of our Milky Way model: the mass of the disc $M_{\rm d}$ and bulge $M_{\rm b}$, the dark matter density $\rho_{\rm h}$, and $r_{\rm h}$. In this way we recover $M_{\rm d} = 5.3^{+1.29}_{-1.71} \times 10^{10}{\rm M}_\odot$ and $M_{\rm b} = 2.49^{+0.44}_{-0.42} \times 10^{10}{\rm M}_\odot$ in good agreement with our fiducial values of $5 \times 10^{10}{\rm M}_\odot$ and $2.6 \times 10^{10}{\rm M}_\odot$ respectively. Note, that in our simulation there are no EM counterparts beyond $R = 11$ kpc (see Fig. 4). This limits our ability in constraining Milky Way's dark matter halo, indicating that priors on the halo parameters are required. Alternatively, GW detections in globular clusters may add more multi-messenger observations points at $R > 10$ kpc to the rotation curve (e.g., Kremer *et al.*, 2018).

4 Conclusions

Here we outlined the ideas of multi-messenger studies with the *Gaia* and LISA space missions using Galactic binaries composed of white dwarf stars. We discussed the updates on the current census of LISA verification sources after the *Gaia* DR2 for a sample of known Galactic binaries. Specifically, parallaxes provided by *Gaia* allowed the determination of distances for 52 known sources. The obtained distances provide essential missing information for predicting their GW signals, and allow us to confirm 13 guaranteed multi-messenger sources. We also illustrate the prospects for tracing the baryonic mass of the Milky Way using GWs in combination with their optical counterparts. We show that in synergy with *Gaia* data, GW measurements will provide competitive mass estimates for the bulge and stellar disc. However, the choice to use GW sources and their EM counterparts limits our ability to constrain the DM halo component of the Galaxy. This highlights the importance of a more precise knowledge of the DM halo to improve baryonic mass measurements. Thus, we stress that exploring multi-messenger synergies will guarantee the best science return of the LISA mission!

Acknowledgments

This work presents results from the European Space Agency (ESA) space mission Gaia. Gaia data is being processed by the Gaia Data Processing and Analysis Consortium (DPAC). Funding for the DPAC is provided by national institutions, in particular the institutions participating in the Gaia MultiLateral Agreement (MLA). The Gaia mission website is `https://www.cosmos.esa.int/gaia`. The Gaia archive website is `https://archives.esac.esa.int/gaia`. We also acknowledge DPAC for developing PyGaia python tool kit that we used to simulate Gaia data. This work was supported by NWO WARP Program, grant NWO 648.003004 APP-GW.

References

Amaro-Seoane, P., Audley, H., Babak, S., Baker, J., Barausse, E., *et al.* 2017, arXiv e-prints.

Bailer-Jones, C. A. L. 2015, PASP, 127, 994.

Barausse, E., Yunes, N., & Chamberlain, K. 2016, Physical Review Letters, 116, 241104.

Bellm, E. 2014, In *The Third Hot-wiring the Transient Universe Workshop*, edited by P. R. Wozniak, M. J. Graham, A. A. Mahabal, & R. Seaman, pp. 27–33.

Berti, E., Sesana, A., Barausse, E., Cardoso, V., & Belczynski, K. 2016, Physical Review Letters, 117, 101102.

Binney, J. & Tremaine, S. 2011, *Galactic Dynamics: (Second Edition)*. Princeton Series in Astrophysics (Princeton University Press). ISBN 9781400828722.

Bloemen, S., Groot, P., Nelemans, G., & Klein-Wolt, M. 2015, In *Living Together: Planets, Host Stars and Binaries*, edited

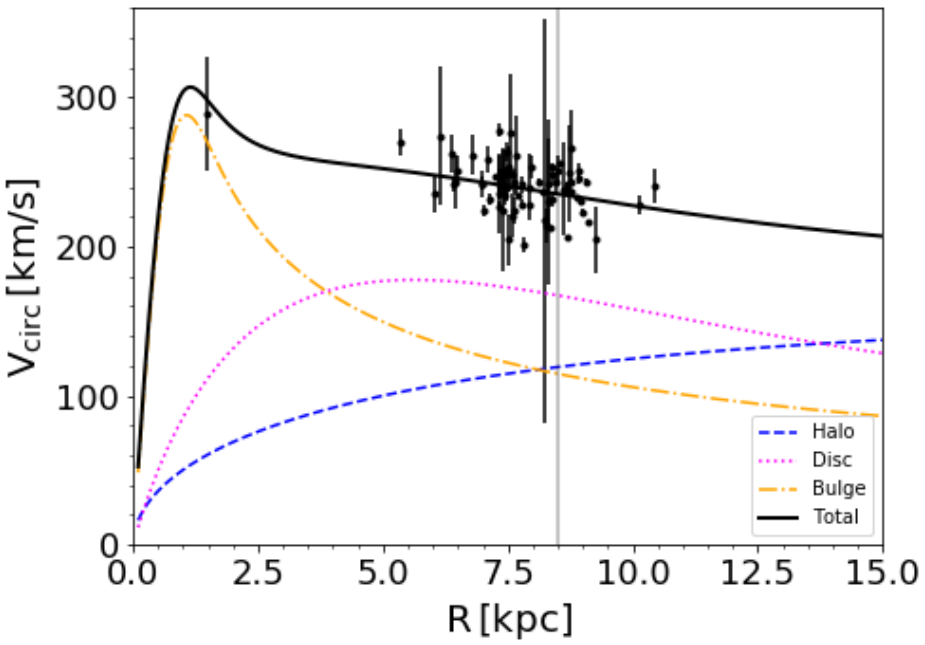

Figure 4: A multi-messenger rotation curve of the Milky Way: R represents Galactocentric cylindrical distance computed by combining distances from GW data with parallaxes, and $V_{\rm circ}$ is the rotation speed of EM counterparts computed using proper motions. Black points represent mock data. The black solid line is the theoretical total rotation curve, while coloured lines represent the contribution of different Galactic components: dark matter halo, stellar disc and bulge. Figure adopted from Korol *et al.* (2019).

by S. M. Rucinski, G. Torres, & M. Zejda, *Astronomical Society of the Pacific Conference Series*, vol. 496, p. 254.
Boissier, S. & Prantzos, N. 1999, MNRAS, 307, 857.
Breivik, K., Kremer, K., Bueno, M., Larson, S. L., Coughlin, S., *et al.* 2018, ApJL, 854, L1.
Brito, R., Ghosh, S., Barausse, E., Berti, E., Cardoso, V., *et al.* 2017, Physical Review Letters, 119, 131101.
Brown, W. R., Kilic, M., Hermes, J. J., Allende Prieto, C., Kenyon, S. J., *et al.* 2011, ApJL, 737, L23.
Brown, W. R., Kilic, M., Kenyon, S. J., & Gianninas, A. 2016, ApJ, 824, 46.
Caprini, C., Hindmarsh, M., Huber, S., Konstandin, T., Kozaczuk, J., *et al.* 2016, , 4, 001.
Carrasco, J. M., Catalán, S., Jordi, C., Tremblay, P.-E., Napiwotzki, R., *et al.* 2014, A&A, 565, A11.
Espaillat, C., Patterson, J., Warner, B., & Woudt, P. 2005, PASP, 117, 189.
Gaia Collaboration, Brown, A. G. A., Vallenari, A., Prusti, T., de Bruijne, J. H. J., *et al.* 2018, A&A, 616, A1.
Gaia Collaboration, Prusti, T., de Bruijne, J. H. J., Brown, A. G. A., Vallenari, A., *et al.* 2016, A&A, 595, A1.
Geier, S., Marsh, T. R., Wang, B., Dunlap, B., Barlow, B. N., *et al.* 2013, A&A, 554, A54.
Green, M. J., Hermes, J. J., Marsh, T. R., Steeghs, D. T. H., Bell, K. J., *et al.* 2018, ArXiv e-prints.
Holberg, J. B. & Bergeron, P. 2006, AJ, 132, 1221.
Jonker, P. G., Bassa, C. G., Nelemans, G., Steeghs, D., Torres, M. A. P., *et al.* 2011, VizieR Online Data Catalog, 219.
Kilic, M., Brown, W. R., Gianninas, A., Hermes, J. J., Allende Prieto, C., *et al.* 2014, MNRAS, 444, L1.
Korol, V., Rossi, E. M., & Barausse, E. 2019, MNRAS, 483, 5518.
Korol, V., Rossi, E. M., Groot, P. J., Nelemans, G., Toonen, S., *et al.* 2017, MNRAS, 470, 1894.
Kowalski, P. M. & Saumon, D. 2006, ApJL, 651, L137.
Kremer, K., Chatterjee, S., Breivik, K., Rodriguez, C. L., Larson, S. L., *et al.* 2018, Physical Review Letters, 120, 191103.
Kupfer, T., Groot, P. J., Bloemen, S., Levitan, D., Steeghs, D., *et al.* 2015, MNRAS, 453, 483.
Kupfer, T., Korol, V., Shah, S., Nelemans, G., Marsh, T. R., *et al.* 2018, MNRAS, 480, 302.
Lamberts, A., Garrison-Kimmel, S., Hopkins, P. F., Quataert, E., Bullock, J. S., *et al.* 2018, MNRAS, 480, 2704.
Littenberg, T. B., Larson, S. L., Nelemans, G., & Cornish, N. J. 2013, MNRAS, 429, 2361.
LSST Science Collaboration, Abell, P. A., Allison, J., Anderson, S. F., Andrew, J. R., *et al.* 2009, ArXiv e-prints.
Luri, X., Brown, A. G. A., Sarro, L. M., Arenou, F., Bailer-Jones, C. A. L., *et al.* 2018, ArXiv e-prints.
Maggiore, M. 2008, *Gravitational waves: theory and experiments* (Oxford: Oxford Univ. Press).
Nelemans, G., Yungelson, L. R., & Portegies Zwart, S. F. 2001, A&A, 375, 890.
Nelemans, G., Yungelson, L. R., & Portegies Zwart, S. F. 2004, MNRAS, 349, 181.
Nissanke, S., Vallisneri, M., Nelemans, G., & Prince, T. A. 2012, ApJ, 758, 131.
Portegies Zwart, S. F. & Verbunt, F. 1996, A&A, 309, 179.
Ramsay, G., Hakala, P., Wu, K., Cropper, M., Mason, K. O., *et al.* 2005, MNRAS, 357, 49.

Roelofs, G. H. A., Groot, P. J., Benedict, G. F., McArthur, B. E., Steeghs, D., *et al.* 2007, ApJ, 666, 1174.
Roelofs, G. H. A., Groot, P. J., Marsh, T. R., Steeghs, D., & Nelemans, G. 2006, MNRAS, 365, 1109.
Ruiter, A. J., Belczynski, K., Benacquista, M., Larson, S. L., & Williams, G. 2010, ApJ, 717, 1006.
Schlegel, D. J., Finkbeiner, D. P., & Davis, M. 1998, ApJ, 500, 525.
Shah, S., Nelemans, G., & van der Sluys, M. 2013, A&A, 553, A82.
Shah, S., van der Sluys, M., & Nelemans, G. 2012, A&A, 544, A153.
Sofue, Y. 2017, , 69, R1.
Steeghs, D. 2017, Nature Astronomy, 1, 741.
Ströer, A. & Vecchio, A. 2006, Classical and Quantum Gravity, 23, 809.
Strohmayer, T. E. 2004, ApJL, 608, L53.
Tamanini, N., Caprini, C., Barausse, E., Sesana, A., Klein, A., *et al.* 2016, , 4, 002.
Tauris, T. M. 2018, Physical Review Letters, 121, 131105.
Thorstensen, J. R. 2003, AJ, 126, 3017.
Thorstensen, J. R., Lépine, S., & Shara, M. 2008, AJ, 136, 2107.
Toonen, S., Nelemans, G., & Portegies Zwart, S. 2012, A&A, 546, A70.
Tremblay, P.-E., Bergeron, P., & Gianninas, A. 2011, ApJ, 730, 128.